

DESIGN AND OPTIMIZATION OF DYNAMIC CABLE CONFIGURATION DEVICE FOR INTELLIGENT CABLE RETRACTABLE VEHICLE

ZHANLONG LI, ZHIZHAO REN

School of Vehicle and Transportation Engineering, Taiyuan University of Science and Technology, Taiyuan, China, and Shanxi Intelligent Transportation Laboratory Co., Ltd., Taiyuan, China

corresponding author Zhanlong Li, Zhizhao Ren, e-mail: lizl@tyust.edu.cn, 1529067216@qq.com

HUI WANG, ZHENG ZHANG

School of Vehicle and Transportation Engineering, Taiyuan University of Science and Technology, Taiyuan, China, and Smart Transportation Laboratory in Shanxi Province, Taiyuan, China

BEIJUN GUO

Technology Center, Shanxi Jiacheng Hydraulic Co., Ltd., Yuanping, China

A new mining dynamic cable configuration device has been designed with adjustable cable curvature, full-range guiding restriction, and an anti-dragging warning function to improve the intelligence level and multi-scenario applicability. The digital model of the dynamic cable configuration device is constructed, and a theoretical formula for interactions between its structure parameters, assembly parameters, and the cabling work state is deduced. Strength analysis and topology optimization reconstruction of the side plate of the dynamic cable configuration device are carried out by using Ansys. The intelligent cable retractable device has been successfully applied in engineering. These research results can provide a theoretical basis for cooperative regulation and intelligent upgrading of both mining dynamic cable configuration devices and intelligent cable retractable devices.

Keywords: mechanical engineering, dynamic cable configuration device, mathematic model, topology optimization

1. Introduction

Mining electric shovels are indispensable equipment for large-scale open-pit mines in stripping operations (Topno *et al.*, 2021; Wang *et al.*, 2023). Their workload accounts for more than 50% of the total workload. Due to the requirements of high-power and continuous excavation, electric shovels often operate with high-voltage electricity (6000 V-10000 V) delivered by cables as a real-time power source. The reliability of the cable power supply directly affects the efficiency of excavation and mining operations (Zhao, 2023). Currently, electric shovels mainly use intelligent cable retractable devices to wind and unwind high-voltage cables during stripping operations in large-scale open-pit mines. Given the weight and bending radius of mining high-voltage cables, as well as frequent operation of the cable winding equipment, a dynamic cable configuration device is typically used to assist coordinated take-up and take-down by the reel (Han *et al.*, 2012; Amnuanpol, 2019).

The rationality, intelligence, and lightweight level of the structural design of the dynamic cable configuration device are crucial for ensuring reliable cabling work as an important component of an intelligent cable retractable device. However, there are several issues in the current application process of mining dynamic cable configuration devices on the market. (1) The dynamic cable configuration device lacks accuracy in following the reel assembly, which leads to cable accumulation or disorder (in Fig. 1a), resulting in uneven cable arrangement and heat

buildup, which reduces the capacity and service life of the cables. (2) Unreasonable design parameters of the dynamic cable configuration device can cause wear, bending, or even breakage of cables while also reducing precision in screw drive (in Fig. 1b) (Kevac *et al.*, 2017). (3) There is a lack of effective warning devices; therefore, the cables are susceptible to scraping and pressing by rocks and coal in unstructured pavement environments found in open-pit mines. Additionally, an excessive force from a large reel can lead to safety hazards such as cable breakage and leakage (Sun *et al.*, 2022). Therefore, it is essential to investigate how structural and assembly parameters influence stability within the dynamic cable configuration devices to enhance their applicability across various scenarios while prolonging their service life.

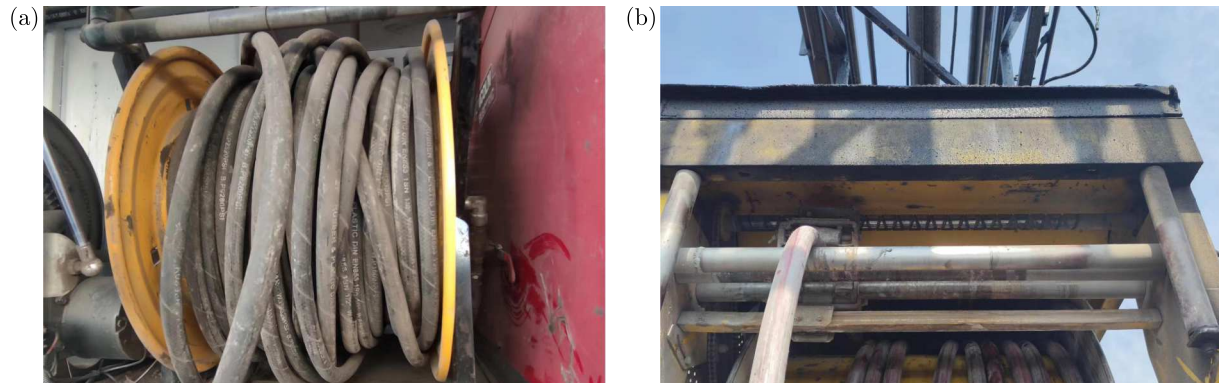


Fig. 1. Application status: (a) cable accumulation or confusion, (b) local deformation of the screw

Wang (2022) used Ansys to analyze how different positions of guide wheels affect the strength of the dynamic cable configuration device during sailing and towing conditions. The results showed that the maximum force and deformation occurred when the guide wheels were in middle positions under both conditions, providing insights into strength analysis and verification for similar types of dynamic cable configuration devices. Kevac *et al.* (2017) introduced dynamic variables such as winding/unwinding radius and cable length, considering their impact on the dynamic response of cable winding/unwinding systems, and defined a general form for mathematical models of cable winding/unwinding systems. In the same year, Kevac and Filipovic (2017) conducted a comprehensive analysis and characterization of nonlinear and pulsating phenomena associated with the radial multi-layer winding process on winches, extending its applicability to studying rope winding processes in complex systems. These research studies establish a fundamental framework for structural design and parameter optimization of dynamic cable configuration devices under challenging mining conditions. Concurrently, topology optimization based on the variable density approach, which utilizes strain energy as the objective function and volume as the constraint function, has gradually emerged as a pivotal technique for automated design across diverse industries such as automotive, mechanical, and aerospace sectors since its introduction by Bendsoe and Kikuchi (1988). Notably, this approach is extensively employed in lightweight design of structures, offering an effective means for weight reduction and reconstruction design of cable winders (Zhang *et al.*, 2007).

Therefore, to address the aforementioned issues, this study initially proposes the design of a novel mining dynamic cable configuration device featuring adjustable cable curvature, full-range guiding restriction, and an anti-dragging warning function, aimed to enhance the quality and stability of cabling operations. Subsequently, a mathematical model is established to examine the effects of cable arrangement structure and assembly parameters on the device performance, thereby providing a reliable parameter influence law for the structural design and assembly position determination of the device. Finally, based on strength analysis results of the device side plate, the topology optimization module Ansys is employed to reconstruct the side plates

in effort to reduce the influence of device quality on the stability of the screw and the improve unit mass-bearing capacity under various working conditions.

2. Dynamic cable configuration device

The intelligent cable retractable device is positioned at the front of the intelligent cable retractable vehicle, which consists of the frame assembly, reel assembly, power system, transmission system, dynamic cable configuration device, etc. Power is transmitted to the reel and reciprocating screw-screw pair through the transmission device. This enables it to work in conjunction with the chassis system to realize safe and stable operation for functions such as “active cable winding, passive cable discharging and in situ cable winding and discharging”, as shown in Fig. 2. One end of the dynamic cable configuration device is placed on the guiding rod by means of a guiding wheel set, and the other end is connected to the reciprocating screw through the screw pair. It serves as a key device for the intelligent cable retractable device to realize an even arrangement and stable unwinding of the cables.

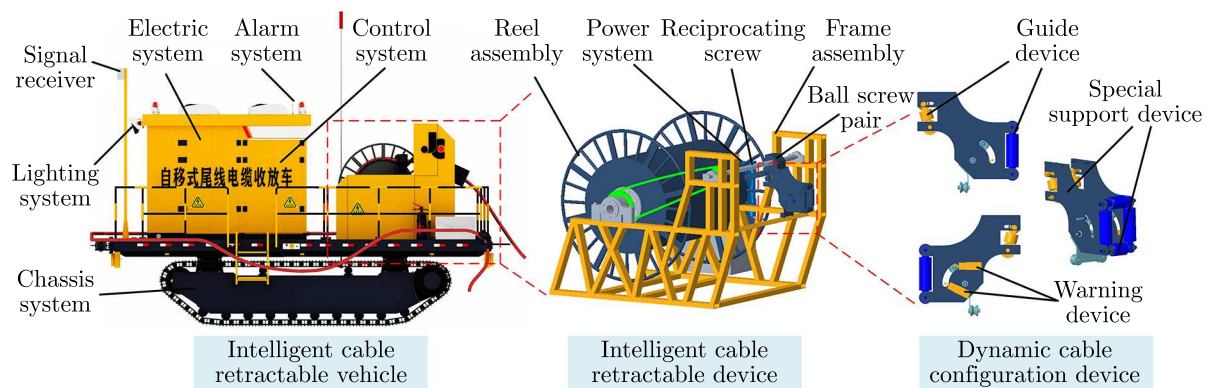


Fig. 2. Intelligent cable retractable device

2.1. Dynamic cable configuration device structure

The dynamic cable configuration device consists of three parts: the guide device, special support device and warning device, as shown in Fig. 3. Among them, the guide device works through

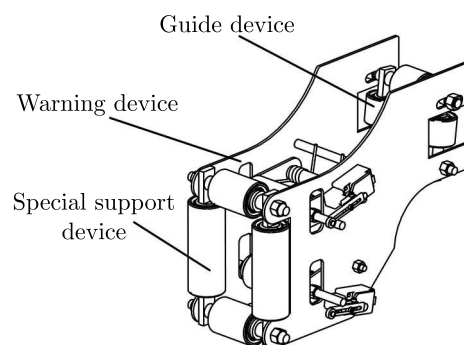


Fig. 3. Dynamic cable configuration device

synergistic cooperation of each roller to provide full-range cable guidance; the special support device has characteristics of strong loading-impact resistance, compatibility with multiple types of cables, and good alignment characteristics, which can realize stable arrangement of cables in the process of winding and releasing. By monitoring cable tension, the warning device can switch

between three working states of the cabling work – warning and emergency shutdown – while providing anti-dragging warnings to prevent cable bending or breaking due to overstretching. Additionally, the dynamic cable configuration device is fixed on the reciprocating screw pair for left-right translation and automatic reversing. The mechanical structure transmission mode of the reciprocating screw-screw pair ensures uniform cable arrangement and improves cabling work stability.

The dynamic cable configuration device possesses characteristics of anti-dragging warning and adjustable cable bending radius. With the addition of a control system, it can achieve intelligent monitoring and warning of the state of the dynamic cable configuration device, as well as adaptive adjustment of the bending radius. This feature allows for excellent adaptability to the intelligent cable retractable device, and is highly significant for construction of intelligent mines.

2.2. Guide device

The guide device is divided into a front guide device and a rear guide device, which are composed of lateral rollers and transverse rollers. The lateral and transverse rollers are in the same plane. During the cable movement process, they can play a role in guiding and protecting the full range of the cable. Each roller consists of a smooth roller and rolling bearings. By cooperating with each roller, the friction coefficient can be reduced to minimize cable wear, as shown in Fig. 4.

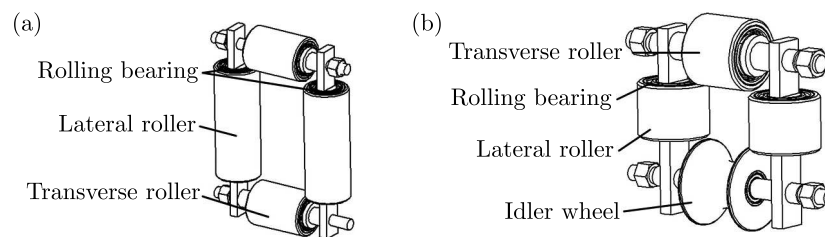


Fig. 4. Guide device: (a) front guide device, (b) rear guide device

By setting up a rotating arm structure, the rear guide device can adjust its angle according to the maximum bending coefficient of different cable specifications, and then adjust the bending radius of the input cable to adapt to different types of cables.

2.3. Special support device

The special support device comprises a front support roller assembly and a rear support roller assembly, which can realize the uniform arrangement of cables during cable installation operation. Moreover, the special support device exhibits robust loading-impact resistance and compatibility with various cable types while ensuring precise alignment. Consequently, it can accommodate diverse cable-supporting needs effectively. Withstanding up to 10 meters of the cable (weighing 6.9 kg/m), its exceptional stability guarantees compliance with overall stiffness and strength requirements, as depicted in Fig. 5.

2.4. Warning device

The warning device consists of the upper and lower stroke switch, rocker, and torsion spring. Through cooperation of the torsion spring with the rocker, the upper and lower stroke switch can be triggered, allowing for feedback on the state signal of the dynamic cable configuration device to be sent back to the controller. This enables obtaining information about cable tautness state

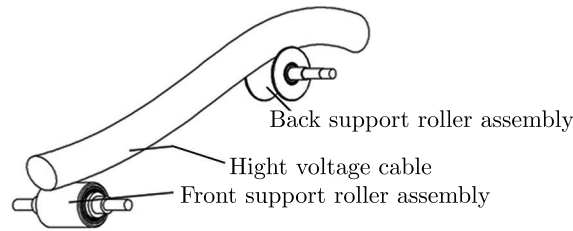


Fig. 5. Special support device

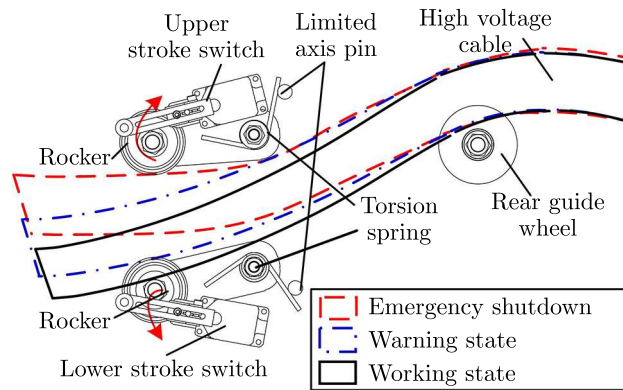


Fig. 6. Warning device

in order to regulate three working states of the cabling work, warning and emergency shutdown, as shown in Fig. 6.

- Working state: the contact between the cable and the rocker triggers the action of the lower stroke switch, and the dynamic cable configuration device runs normally;
- Warning state: the cable is lifted by resistance and separated from the rocker, but the upper and lower stroke switch are not triggered. At this time, the cable is subjected to a large tension, but not more than the maximum permissible tension, and the system gives a warning;
- Emergency shutdown: the resistance of the cable continues to increase, and the cable lifts to contact the upper rocker, triggering the upper stroke switch. At this point, the tension of the cable is greater than the maximum permissible tension, and the system stops in emergency to protect the cable from excessive tension damage.

3. Characteristics of parameter interaction

The structure parameters, assembly parameters, and performance indicators of the dynamic cable configuration device are interconnected. Studying the interaction law of each parameter is a prerequisite for optimizing and transforming the dynamic cable configuration device.

3.1. Design parameters of the dynamic cable configuration device

Figure 7 shows a schematic diagram of the movement principle of the dynamic cable configuration device when the intelligent cable retractable device is used for a high-voltage cable retracting and releasing work. In Fig. 7, α_1 is the angle between the suspended cable and horizontal direction, which can be set according to operating conditions; α_2 is the angle between the horizontal direction and connecting line (between the reel center and the lower roller center of the special support device); α_3 is the angle between the connecting line (between the center of

the reel and lower roller center of the special support device) and tangent line (between the reel and lower roller of the special support device); α_4 is the angle between horizontal direction and connecting line (between the lower roller center of the special support device and guide device roller center); β_1 is the angle between the cable of segment AB and segment BC ; β_2 is the angle between the cable of segment AB and suspended cable; γ_1 is the angle between the vertical direction and resultant force on the lower roller of the guide device; γ_2 is the angle between the vertical direction and resultant force on the lower roller of the special support device.

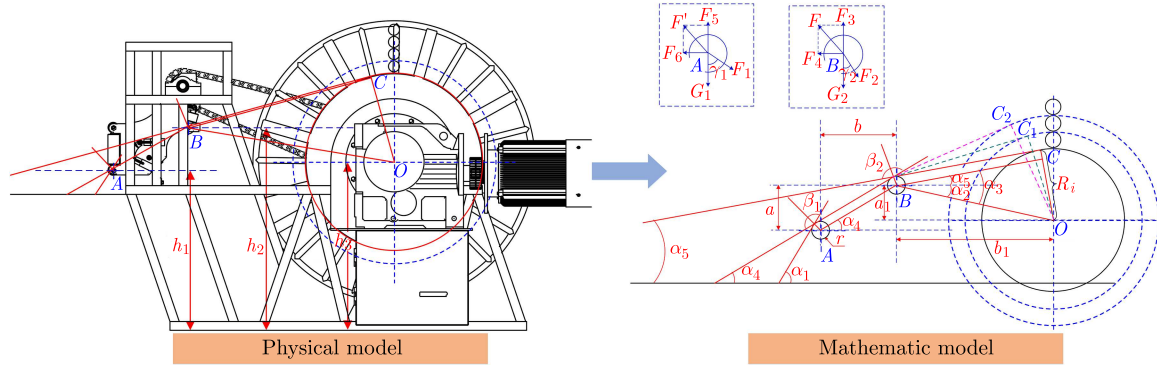


Fig. 7. Working model of the intelligent cable retractable device

Based on the geometric relationship in Fig. 7, when the dynamic cable configuration device is used to arrange a cable, an expression between the structure parameters, assembly parameters, and position parameters of each segment of the cable can be obtained

$$\alpha_2 = \arctan \frac{a_1}{b_1} \quad \alpha_3 = \arcsin \frac{R_i - r}{\sqrt{a_1^2 + b_1^2}} \quad (3.1)$$

$$\alpha_4 = \arctan \frac{a}{b} \quad \alpha_5 = \alpha_3 - \alpha_2$$

and

$$\beta_1 = \pi - \alpha_1 + \alpha_4 \quad \beta_2 = \pi - \alpha_4 + \alpha_5 \quad (3.2)$$

and

$$\gamma_1 = \frac{\beta_1}{2} - \left(\frac{\pi}{2} - \alpha_1\right) \quad \gamma_2 = \frac{\beta_2}{2} - \left(\frac{\pi}{2} - \alpha_4\right) \quad (3.3)$$

where a_1 and b_1 are the vertical and horizontal distances between the lower roller center of the special support device and the center of the reel, a and b are the vertical and horizontal distances between the lower roller center of the special support device and the lower roller center of the guide device, R_i ($i = 1, 2, 3, \dots$) is the radius when winding i -layers of the cable on the reel, R_1 is equal to the reel radius, r is the radius of the roller of the dynamic cable configuration device.

When the number of cable layers on the reel changes, the expression for R_i is as follows

$$R_i = R_1 + (i - 1)d \quad (3.4)$$

where d is the diameter of the high-voltage cable.

The cable of segments AB and BC are approximately arranged in a straight line, when a pre-tightening force is applied by the intelligent cable retractable device. Therefore, the cable

bending radius λ can be determined from the length and angle parameters of the cable in segments AB and BC

$$\begin{aligned} l_{BC} &= \frac{R_i - r}{\tan \alpha_3} & l_{AB} &= \frac{a}{\sin \alpha_4} & l_{AC} &= l_{AB}^2 + l_{BC}^2 - 2l_{BC}l_{AB} \cos \beta_2 \\ \lambda &= \frac{l_{AC}}{2 \sin \beta_2} \end{aligned} \quad (3.5)$$

where l_{AB} and l_{BC} are the lengths of the cable in segments AB and BC .

At the same time, the warning state of the warning device depends on the structure parameters a and b . When $\alpha_4 = \alpha_1$, the lower stroke switch is disconnected and the warning is activated.

The structure parameters and assembly parameters of the dynamic cable configuration device are designed as listed in Table 1.

Table 1. Structure parameters of the cable arrangement device

Parameter	Value	Parameter	Value
a_1 [mm]	193	α_1 [°]	60
b_1 [mm]	1163.5	d [mm]	65
a [mm]	240.5	d_1 [mm]	40
b [mm]	423	g [m/s ²]	9.8
R_1 [mm]	534	r [mm]	32.5

Substituting the parameter values from Table 1 into Eq. (3.1) to (3.5) one can obtain.

Table 2. Position parameters of cable arrangement device

Parameters	$i = 1$	$i = 2$	$i = 3$
α_2 [°]	9.42	9.42	9.42
α_3 [°]	25.16	28.71	32.37
α_4 [°]	29.62	29.62	29.62
β_1 [°]	149.62	149.62	149.62
β_2 [°]	166.13	169.67	173.33
γ_1 [°]	44.81	44.81	44.81
γ_2 [°]	22.68	24.45	26.28
λ [mm]	4972410	6404040	9441800

From Table 2, it can be observed that during the operation of the dynamic cable configuration device, α_3 , β_2 and γ_2 will vary with the number of cable layers arranged on the reel, primarily affecting the working environment of the lower roller of the special support device. Simultaneously, a bending radius 15 times greater than the diameter of the cable is required for proper functioning. Based on the data in Table 2, increasing the number of cable layers proves to be advantageous in enhancing the high-voltage cables working environment.

3.2. Mechanical characteristics of the dynamic cable configuration device

The force analysis of the guide device roller and the special support roller is shown in Fig. 7, when the cable is arranged on the reel. The equilibrium equations of the two rollers are obtained

$$F_1 = 2F_s \cos \frac{\beta_1}{2} \quad F_2 = 2F_s \cos \frac{\beta_2}{2} \quad F_s = \frac{G_s}{\tan \alpha_1} \quad (3.6)$$

and

$$F_5 = G_1 + F_1 \cos \gamma_1 \quad F_6 = F_1 \sin \gamma_1 \quad F' = \sqrt{F_5^2 + F_6^2} \quad (3.7)$$

and

$$F_3 = G_2 + F_2 \cos \gamma_2 \quad F_4 = F_2 \sin \gamma_2 \quad F = \sqrt{F_3^2 + F_4^2} \quad (3.8)$$

where F_1 and F_2 are the resultant forces acting on the guide device roller and the special support roller, F_4 and F_3 are the vertical and horizontal components of the force F on the reciprocating screw, F_5 and F_6 are the vertical and horizontal components of the force F' on the guiding rod, m is mass of the dynamic cable configuration device, F_s is the tensile force on the cable, G_s is the gravity force acting on the suspended cable, $G_2 = G_1 = mg/2$.

The contact length between the reciprocating screw and the screw pair is much smaller than the length of the reciprocating screw, so the force on the reciprocating screw can be simplified to the concentrated force. Additionally, since the length of the reciprocating screw is much larger than its section diameter, we can neglect the effect of the shear force on bending deformation (Tang *et al.*, 2022). Based on the plane assumption that the cross-section perpendicular to the axis remains perpendicular to the deflection curve after deformation, a force analytical model for the reciprocating screw is established with the axis of the screw before deformation as the x -axis, the vertical direction as the y -axis, and the longitudinal symmetry plane of the screw as the xy plane, as shown in Fig. 8.

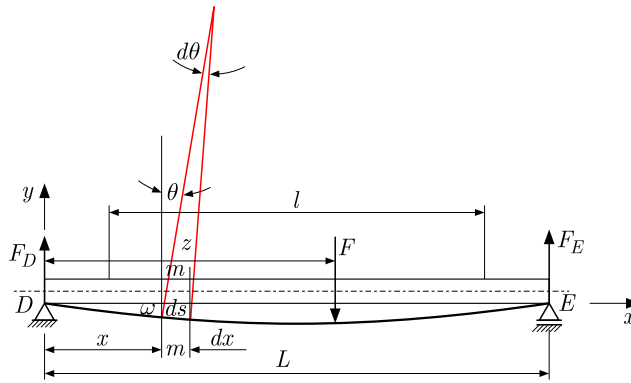


Fig. 8. Force analytical model for the reciprocating screw

Using the static equilibrium equation, the support constraints at the ends D and E of the reciprocating screw are obtained

$$F_D = \frac{F(L - z)}{L} \quad F_E = \frac{Fz}{L} \quad (3.9)$$

where L is the length of the reciprocating screw, z is the x -axis coordinate value of the screw pair, which varies within the effective length l of the reciprocating screw.

The bending moment equation for any point of the reciprocating screw is obtained in segments

$$M(x) = \begin{cases} \frac{F(L - z)}{L}x & \text{for } 0 \leq x \leq z \\ \frac{Fz}{L}(L - x) & \text{for } z \leq x \leq L \end{cases} \quad (3.10)$$

Due to small deformation of the reciprocating screw, a differential equation for the deflection curve of the reciprocating screw is established (Gere and Timoshenko, 1984)

$$\frac{d^2\omega}{dx^2} = \frac{M}{EI} \quad (3.11)$$

where $I = \pi d_1^4/64$ is the cross-section moment of inertia of the screw relative to the centroid axis, d_1 is the diameter of the reciprocating screw, ω is the displacement of the centroid of the cross-section with coordinates x along the y -direction, which is the deflection, E is the elastic modulus of the reciprocating screw, 210 GPa.

The substitution of Eq. (3.10) into Eq. (3.11) yields

$$EI\omega(x) = \begin{cases} \frac{F(L-z)}{6L}x^3 + C_1x + D_1 & \text{for } 0 \leq x \leq z \\ \frac{Fz}{2}x^2 - \frac{Fzx^3}{6L} + C_2x + D_2 & \text{for } z \leq x \leq L \end{cases} \quad (3.12)$$

According to the continuity condition, when $x = z$, the first derivative of the deflection with respect to the deflection at the segmental point corresponds to equality. From the boundary conditions, for $x = 0$ or $x = L$, $\omega = 0$, we obtain

$$\omega(x) = \begin{cases} \frac{Fx[2L^2z + z(x^2 + z^2) - L(x^2 + 3z^2)]}{6LEI} & \text{for } 0 \leq x \leq z \\ \frac{Fz[2L^2x + x(x^2 + z^2) - L(z^2 + 3x^2)]}{6LEI} & \text{for } z \leq x \leq L \end{cases} \quad (3.13)$$

By using Eqs. (3.8) and (3.13), a sensitivity expression for screw deflection to the mass change of the dynamic cable configuration device is obtained

$$S = \frac{d\omega}{dm} \frac{m}{\omega} = -\frac{gm\left(\frac{mg}{2} + F_2 \cos \gamma_2\right)}{2\left[\left(\frac{mg}{2} + F_2 \cos \gamma_2\right)^2 + (F_2 \sin \gamma_2)^2\right]} \quad (3.14)$$

Based on the measured values ($m = 30$ kg and $G_s = 690$ N), the data in Tables 1 and 2 are substituted into Eq. (3.14) to obtain $S = -0.48$, which means that the mass of the dynamic cable configuration device is reduced by 20%, and the maximum screw deflection is reduced by 9.6%.

At the same time, the number of retracted cable meters is directly proportional to the tension F_s on the cable, when the intelligent cable retractable device retracts the cable in situ. An increase of F_s will change the load-bearing state of the dynamic cable configuration device. In order to comprehensively describe its state under different loads, we define the mass utilization coefficient as the load borne by the unit mass. When this coefficient exceeds a certain limit value, it indicates that the dynamic cable configuration device is in an overloaded working state. When it is lower than a certain limit value (at this time $\alpha_4 = \alpha_1$), it indicates that the dynamic cable configuration device is in a warning working state. Under conditions satisfying strength and stiffness, a higher mass utilization coefficient implies greater utilization per unit mass, making for a more economical and reasonable structure of the dynamic cable configuration device

$$P = \frac{F_f}{m} \quad (3.15)$$

where P is the mass utilization coefficient, F_f is the load of the dynamic cable configuration device. The expression for F_f is obtained

$$F_f = \sqrt{(F_1 \cos \gamma_1 + F_2 \cos \gamma_2)^2 + (F_1 \sin \gamma_1 + F_2 \sin \gamma_2)^2} \quad (3.16)$$

By substituting the values from Tables 1 and 2 into Eqs. (3.6), (3.15), and (3.16), it can be concluded that the mass utilization coefficient of the dynamic cable configuration device is 16.58 N/kg, when the intelligent cable retractable device operates in conjunction with the chassis.

4. Strength analysis of side plates of the dynamic cable configuration device

High-voltage cables used in open-pit mines have a high mass per unit length. In order to ensure that the dynamic cable configuration device has sufficient load-bearing capacity under design loads and to guarantee safety and reliability of its structure. Ansys is utilized for static simulation of the side plates of the dynamic cable configuration device based on the 3D model created by Solidworks in this Section (Nie *et al.*, 2011).

The side plates of the dynamic cable configuration device are made of Q235B steel with a Young's modulus of 206GPa, Poisson's coefficient of 0.3, a yield strength of 250 MPa and a tensile strength of 460 MPa. The thickness of the side plates is 5 mm. The vertical upward load is set at 2000 N, and the vertical downward load is set at 700 N. The specific distribution is shown in Fig. 9.

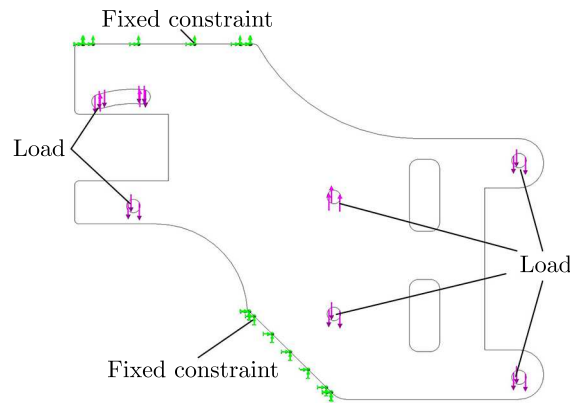


Fig. 9. Schematic of side plates loading

The side plate of the dynamic cable configuration device was statically analyzed to obtain the corresponding stress and strain cloud diagrams, as shown in Fig. 10. Among them, the weight of the side plate is 5.268 kg, and the maximum stress is 30.824 MPa, which is much smaller than the permissible stress of the material and meets both strength and stiffness requirements.

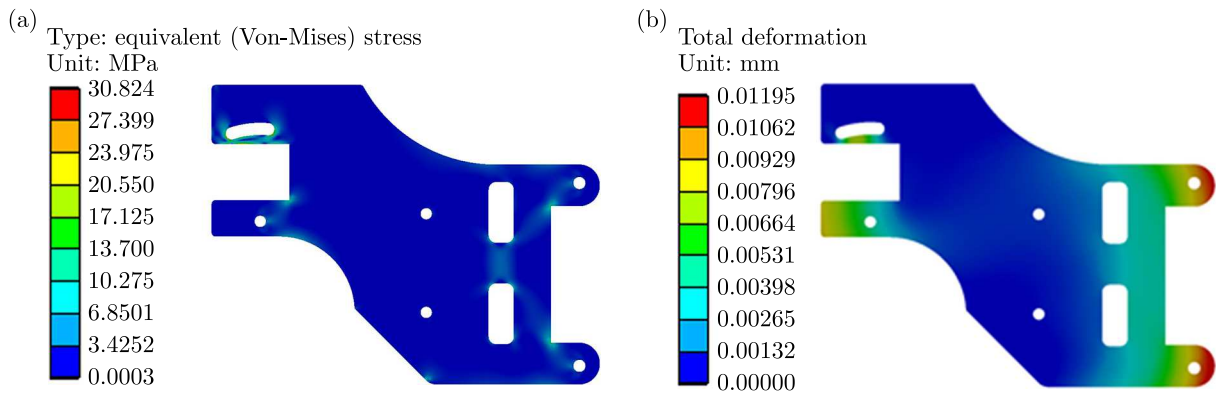


Fig. 10. Stress analysis of the side plates: (a) stress, (b) strain

The safety coefficients are calculated according to

$$N = \frac{[\sigma]}{\sigma} \quad (4.1)$$

where N is the safety coefficient, $[\sigma]$ is the permissible stress, σ is the maximum working stress.

According to Eq. (4.1), $N = 8.11$, the side plates are designed to meet strength requirements.

5. Topology optimization and reconstruction

The accuracy of the reciprocating screw is affected by its stiffness in cabling work. If the deformation is too large, it will affect the precision of the screw and the screw pair, resulting in uneven wear, noise, vibration, and reduced lifespan. The lightweight design of the dynamic cable configuration device is an important method to improve both the precision of cabling work and the mass utilization coefficient of the dynamic cable configuration device. This design also enhances operational efficiency and reduces production costs. In this Section, the topological reconstruction of the side plates for the dynamic cable configuration device is performed based on Ansys.

5.1. Optimization program

Topological optimization can identify the optimal material distribution scheme within the optimization space of a homogeneous material (Song *et al.*, 2017). In this Section, the objective of topology optimization is to minimize strain energy for the overall structure of the side plate, while ensuring that the volume of the optimized side plate does not exceed 40% of its original volume. The mathematical representation of topological optimization is as follows (Radhi *et al.*, 2021)

$$\begin{aligned}
 &\text{find: } \mathbf{x} = [X_1, X_2, \dots, X_n]^T \\
 &\text{min : } C(x) = \frac{1}{2} \mathbf{U}^T \mathbf{K} \mathbf{U} \\
 &\text{s.t. } \left\{ \sum_{i=1}^N V_i X_i \leq V^*; \mathbf{F} = \mathbf{K} \mathbf{U}; X_{min} \leq X_i \leq 1 \ (i = 1, \dots, n) \right\}
 \end{aligned} \tag{5.1}$$

where \mathbf{U} , \mathbf{K} and \mathbf{F} are the displacement vector, global stiffness matrix and load vector, respectively, for the n element domain. The first constraint is a volume constraint to be below a certain value V^* . The second constraint represent the equilibrium condition, from which \mathbf{U} is calculated. Here, a value X_{min} of 0.001 was found to be suitable for our simulations.

5.2. Analysis of optimization results

The optimization analysis converges after 24 iterations, and the topology optimization results are shown in Fig. 11.

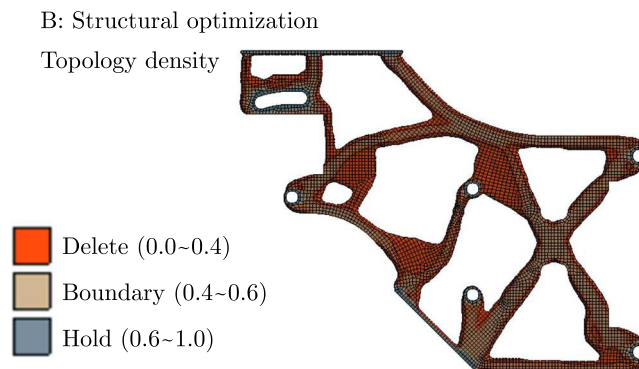


Fig. 11. Topology optimization results

The side plates have been reconstructed based on the topology optimization results, weighing 2.227 kg as depicted in Fig. 12a. By applying the same constraints and loading conditions as the original model for static analysis, the maximum stress is measured at 31.624 MPa with a safety coefficient of 7.9, as shown in Fig. 12b.

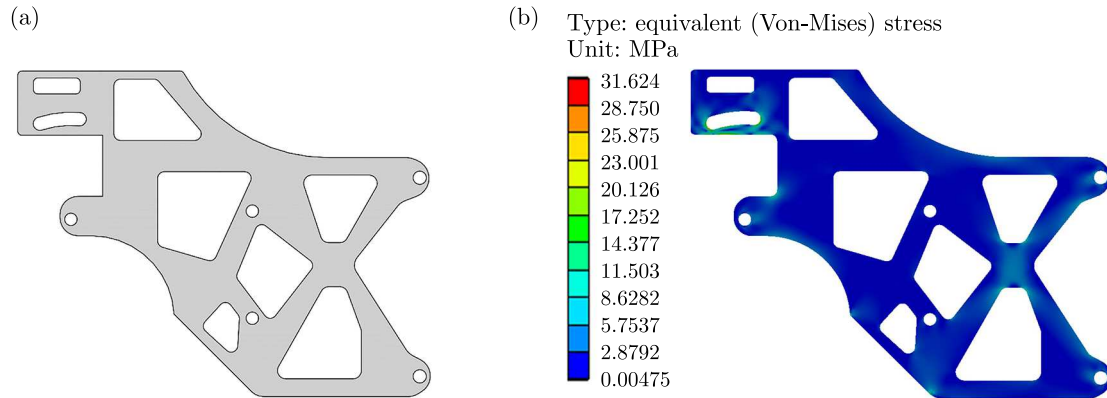


Fig. 12. Reconstructed side plates: (a) side plate model, (b) stress diagram

After reconstruction, the stress on the side plate is much lower than the material yield strength, and the design still has a significant redundancy. Therefore, in the second reconstruction, the thickness of the side plate is reduced to 3 mm. The weight of the side plate after this second reconstruction is 1.670 kg. By applying identical constraints and loading conditions as in the original model for static analysis, we measured a maximum stress of 37.722 MPa with a safety coefficient of 6.62, as shown in Fig. 13.

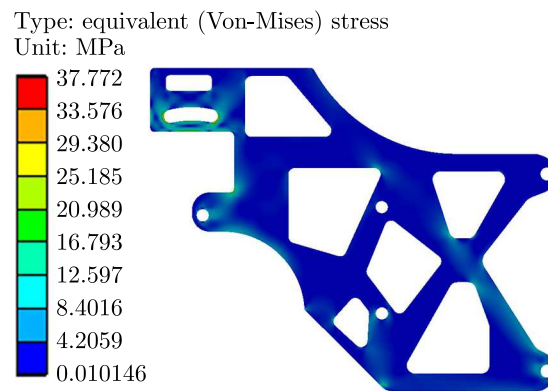


Fig. 13. Stress diagram of the side plates after second reconstruction

5.3. Comparative analysis

As shown in Table 3 and 4, when the thickness of the side plate is taken as 5mm, the weight of the side plate decreases by 57.7% to 2.227 kg, while the maximum stress is reduced to 31.624 MPa. Additionally, the mass of the dynamic cable configuration device decreases by 20.3% to 23.918 kg. When the thickness of the side plate is reduced to 3 mm, its weight decreases by 68.3% down to 1.670 kg and the maximum stress becomes 37.772 MPa. Meanwhile, the mass of the dynamic cable configuration device decreases by 24.0% to 22.804 kg.

To ensure the precision of cabling work and extend equipment service life while reducing operational costs, the weight reduction achieved with a safety coefficient that meets requirements makes the side plate weighing only 1.670kg better fit for lightweight design specifications. The mass utilization coefficient for the dynamic cable configuration device reaches 21.83 N/kg when

Table 3. Comparative advantage

	Deformation	Equivalent (von Mises) stress
Original side plate	<p>Total deformation Unit: mm</p>	<p>Type: equivalent (von Mises) stress Unit: MPa</p>
Optimized side plate (5 mm)	<p>Total deformation Unit: mm</p>	<p>Type: equivalent (von Mises) stress Unit: MPa</p>
Optimized side plate (3 mm)	<p>Total deformation Unit: mm</p>	<p>Type: equivalent (von Mises) stress Unit: MPa</p>

Table 4. Data analysis

Structural element	Weight [kg]	Maximum stress [MPa]	Safety coefficient
Original side plate	5.268	30.824	8.11
Optimized side plate (5 mm)	2.227	31.624	7.9
Optimized side plate (3 mm)	1.670	37.772	6.62

the intelligent cable retractable device works in conjunction with the chassis. This design concept has already been adopted and successfully implemented in large-scale open-pit mine engineering applications, such as showed in Fig. 14.

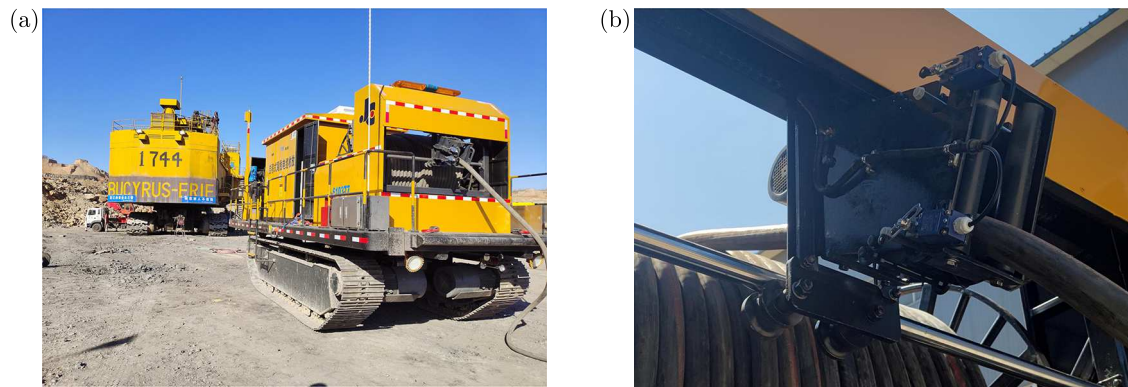


Fig. 14. (a) Intelligent cable retractable vehicle, (b) dynamic cable configuration device

6. Conclusions

This study has developed a novel mining dynamic cable configuration device for mining enterprises, which was designed and optimized based on both the mathematical model of the device and the topological optimization results obtained from Ansys. The engineered application of this mining dynamic cable configuration device has been successfully implemented in a large open-pit mine. During the research process, we have drawn the following conclusions.

- The dynamic cable configuration device is equipped with an adjustable cable bending degree, full-range guiding limit and an anti-dragging warning function, effectively preventing high-voltage cables from being ripped off or bent. This greatly enhances multi-scenario application capability of the intelligent cable retractable vehicle.
- The mathematical expressions and interaction laws of parameters such as cable bending radius and utilization coefficient of the dynamic cable configuration device are theoretically derived, providing a theoretical basis for structural design of this device, determination of assembly positions, and performance optimization.
- After optimization, the weight of the side plate of the dynamic cable configuration device decreased by 68.3%, and the weight of the device decreased by 24.0%. The maximum deflection of the reciprocating screw was reduced by 11.52%. Through actual engineering applications, it has been observed that stability in discharging cables of the device has been significantly enhanced.

Acknowledgements

This research was supported by the Xinzhou City Science and Technology Plan Project – Key Research and Development Plan (Grant No.20220107), the National Natural Science Foundation of China (Grant No. 52272401), the Fundamental Research Program of Shanxi Province (Grant No. 202203021211185), the Shanxi Students' Platform for Innovation and Entrepreneurship Training Program (Grant No. 20230671) and the Guizhou Province Science and Technology Plan Project – Science and Technology Innovation Talent Team (CXTD [2022]015).

References

1. AMNUANPOL S., 2019, Shape sequence of rope coiling on a rotating plane, *EPL (Europhysics Letters)*, **125**, 5, 54001
2. BENDSØE M.P., KIKUCHI N., 1988, Generating optimal topologies in structural design using a homogenization method, *Computer Methods in Applied Mechanics and Engineering*, **71**, 2, 197-224

3. GERE J.M., TIMOSHENKO S.P., 1984, *Mechanics of Materials*, 2nd SI ed., Van Nostrand Reinhold Co., New York
4. HAN Y.Y., ZHANG Z.G., ZHU K.G., 2012, The design on the improvement of the electric scoop-tram's cable arrangement device, *Applied Mechanics and Materials*, **2034**, 229-231
5. KEVAC L., FILIPOVIC M.M., 2017, Mathematical model of cable winding/unwinding system, *Journal of Mechanics*, **35**, 1, 1-13
6. KEVAC L., FILIPOVIC M., RAKIC A., 2017, Dynamics of the process of the rope winding (unwinding) on the winch, *Applied Mathematical Modelling*, **48**, 821-843
7. NIE J.N., WANG H., XIE D.F., 2011, Finite element analysis of drum on the new type self-driven towing machine for cable, *Applied Mechanics and Materials*, **1245**, 55-57, 664-669
8. RADHI A., IACOBELLIS V., BEHDINAN K., 2021, Manipulation of topologically optimized structures using graphic statics, *Materials Design*, **198**, 109286
9. SONG G.H., JING S.K., ZHAO F.L. WANG Y.D., XING H., ZHOU J.T., 2017, Design optimization of irregular cellular structure for additive manufacturing, *Chinese Journal of Mechanical Engineering*, **30**, 5, 1184-1192
10. SUN L.Q., ZHANG X.D., ZENG Q.L., GAO K.D., JIANG K., ZHOU J.W., 2022, Application of a screw conveyor with axial tilt blades on a shearer drum and investigation of conveying performance based on DEM, *Particuology*, **61**, 91-102
11. TANG Z., LI S.Q., HUANG F., YANG J.W., YANG F., *et al.*, 2022, Optimization of a cable support strategy for roadways in coal mines by using the PSO algorithm, *Geotechnical and Geological Engineering*, **40**, 153-163
12. TOPNO S.A., SAHOO L.K., UMRE B.S., 2021, Energy efficiency assessment of electric shovel operating in opencast mine, *Energy*, **230**, 120703
13. WANG Z.Y., 2022, *Dynamics Analysis of the Cable Arrangement System for Full Ocean Depth Geological Winch* (in Chinese), Harbin Engineering University, Harbin
14. WANG Z.W., JIN Z., WANG J., 2023, Maceral and organic geochemical characteristics of the No. 6 coal seam from the Haerwusu Surface Mine, Inner Mongolia, China, *Energy Exploration and Exploitation*, **41**, 5, 1643-1662
15. ZHANG W.H., DAI G.M., WANG F.W., SUN S.P., BASSIR H., 2007, Using strain energy-based prediction of effective elastic properties in topology optimization of material microstructures, *Acta Mechanica Sinica*, **23**, 1, 77-89 .
16. ZHAO S.X., 2023, *Lightweight and Dynamic Characteristic Research of Walking System for Intelligent Cable Retracting and Releasing Machine* (in Chinese), Taiyuan University of Science and Technology, Taiyuan